

# Construction of Lanthanum Vanadate/Functionalized-Boron Nitride Nanocomposite: The Electrochemical Sensor for Monitoring of Furazolidone

Thangavelu Kokulnathan<sup>a, b</sup>, Ghzzai Almutairi<sup>c</sup>, Shen-Ming Chen<sup>a\*</sup>, Tse-Wei Chen<sup>a,d,e</sup>, Faheem Ahmed<sup>f</sup>, Nishat Arshi<sup>g</sup>, Bandar AlOtaibi<sup>c</sup>

<sup>a</sup>*Electroanalysis and Bioelectrochemistry` Lab, Department of Chemical Engineering and Biotechnology, National Taipei University of Technology, Taipei 10608, Taiwan.*

<sup>b</sup>*Department of Electro-Optical Engineering, National Taipei University of Technology, Taipei 10608, Taiwan.*

<sup>c</sup>*National Center for Energy Storage Technologies, King Abdulaziz City for Science and Technology (KACST), Riyadh 12354, Saudi Arabia.*

<sup>d</sup>*Research and Development Center for Smart Textile Technology, National Taipei University of Technology, Taipei 106, Taiwan.*

<sup>e</sup>*Department of Materials, Imperial College London, London, SW7 2AZ, United Kingdom.*

<sup>f</sup>*Department of Physics, College of Science, King Faisal University, P.O Box 400, Hofuf, Al-Ahsa 31982, Saudi Arabia.*

<sup>g</sup>*Department of Basic Sciences, Preparatory Year Deanship, King Faisal University, P.O Box 400, Hofuf, Al-Ahsa 31982, Saudi Arabia*

## Corresponding author

\*E-mail: [smchen78@ms15.hinet.net](mailto:smchen78@ms15.hinet.net)

Tel: +886 2270 17147, Fax: +886 2270 25238.

Number of Pages	6
Number of Figures	5
Number of Table	1

<b>Entry</b>	<b>Table of Contents</b>	<b>Page. No</b>
	Materials, Reagents and Measurements.	<b>S3</b>
	Instruments	<b>S3</b>
	Functionalization of F-BN	<b>S3</b>
	Synthesis of LaV/F-BN nanocomposite	<b>S3</b>
<b>Fig. S1</b>	TEM image of h-BN	<b>S4</b>
<b>Fig. S2</b>	HAADF-STEM of LaV/F-BN nanocomposite	<b>S4</b>
<b>Fig. S3</b>	BET	<b>S5</b>
<b>Fig. S4</b>	CV signals of bare and modified electrodes in the 0.05M PB (pH 7.0) without FZD.	<b>S5</b>
<b>Fig. S5</b>	(A) Selectivity test of LaV/F-BN/RDGCE with the successive addition of 100 $\mu$ M FZD (a) and higher concentration of interfering species (b–s) in 0.05 M PB (pH 7.0). (B) The operational stability of the LaV/F-BN/RDGCE.	<b>S6</b>
<b>Table S1</b>	FZD detection in human blood serum and urine samples.	<b>S6</b>

### ***Materials, Reagents and Measurements.***

Lanthanum (III) nitrate hexahydrate ( $\text{La}(\text{NO}_3)_3 \cdot 6\text{H}_2\text{O}$ ), ammonium metavanadate ( $\text{NH}_4\text{VO}_3$ ), BN, hydroquinone (HQ), ethanol and all other chemicals (including interfering species) were purchased from Sigma-Aldrich and used without further purification. All the solutions in the experiments were prepared with ultrapure double ionized (DI) water.

### ***Instruments***

Field emission scanning electron microscope (FESEM, ZEISS Sigma 300 microscope) and high-resolution transmission electron microscopy (HRTEM, Shimadzu JEM-1200 EX, 200 kV) were used to study the morphology of the as-prepared samples. The composition and crystal structures of the nanomaterials were analyzed by X-ray diffraction (XRD) on an XPERT-PRO diffractometer (PANalytical B.V., The Netherlands) with  $\text{Cu-K}\alpha$  radiation ( $\lambda = 1.5406 \text{ \AA}$ ) in the  $2\theta$  scan range from  $10^\circ$  to  $90^\circ$ . The chemical and surface electronic state of the nanomaterial was scrutinized by X-ray photoelectron spectroscopy (XPS; Thermo scientific multi-lab 2000).

Electrochemical impedance spectroscopy (EIS) measurements were examined by using ZAHNER scientific instruments (THALES software package). Chemical composition of nanocomposite was performed on a Fourier transform infrared analysis (JASCO 6600, FT-IR) spectrophotometer. All the electrochemical measurements were performed on a CHI 750A Electrochemical workstation (CH Instruments (USA)) with a conventional three-electrode system composed of a platinum wire (Pt) as the auxiliary electrode, an Ag/AgCl saturated KCl as reference electrode and a bare or modified glassy carbon working electrode/rotating disk GCE (GCE/ RDGCE), respectively. All the electrochemical experiments were carried out in a nitrogen atmosphere at room temperature.

### ***Functionalization of F-BN***

The F-BN was synthesized by a simple sonochemical approach in this work [61]. The h-BN (5 g) and HQ (0.1 M) were added to 50 mL of DI water by sonochemical method. The precursor was constantly sonicated at room temperature for 1 h. Finally, a white product was collected by centrifugation and washed with DI water. Afterwards, the final sample (F-BN) was dried in an oven at 60 °C for 12 h.

### ***Synthesis of LaV/F-BN nanocomposite***

Briefly, 0.5 M of  $\text{NH}_4\text{VO}_3$  was dissolved in 50 mL of DI water and was stirred for 30 min at a certain temperature. Subsequently, 0.5 M of  $\text{La}(\text{NO}_3)_3 \cdot 6\text{H}_2\text{O}$  was added to the above solution. After stirring for a few minutes, the above mixture was transferred to a 100 mL Teflon lined autoclave and kept at 180 °C for 12 h. After the reaction, the obtained product (LaV) was rinsed several times with DI water/ethanol and collected by centrifugation. Finally, the LaV was dried and calcined at 400 °C for 2 h. F-BN (60%) and LaV (40%) were dispersed in DI water at 50 °C and sonicated for 30 mins to form homogeneous ink. Then, LaV/F-BN nanocomposite was washed for few times and dried at 60°C overnight.

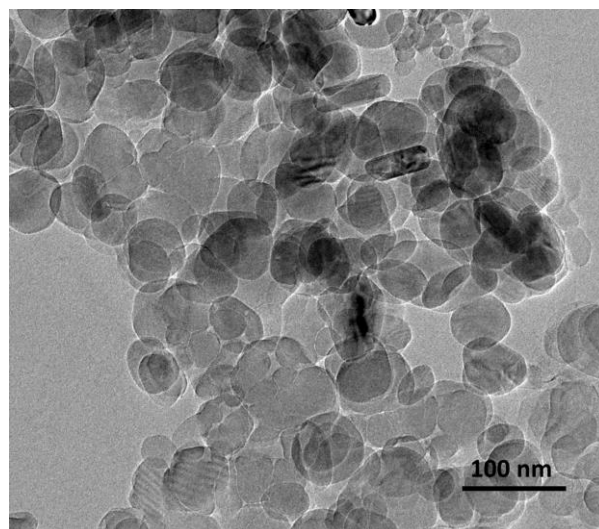


**Fig. S1** TEM image of h-BN.

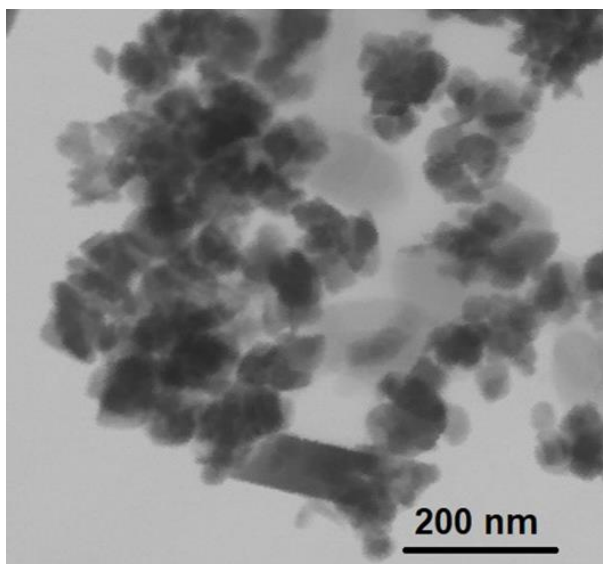


**Fig. S2** HAADF-STEM of LaV/F-BN nanocomposite.

To understand the surface nature in terms of specific surface area BET analysis was carried out. The  $N_2$  - adsorption and desorption isotherms of the samples are given in **Fig. S3**. The isotherms obtained for all three samples could be assigned to type III isotherm, suggests the mesoporous nature of the samples. The measured specific BET surface area of F-BN, LaV and LaV/F-BN is 48.78, 21.98 and 30.56  $m^2 g^{-1}$  respectively. The high specific surface area of F-BN is due to the interspace between the irregular arrangement of F-BNs, which is in agreement with

the TEM images. In comparison with LaV, the larger surface area observed for the LaV/F-BN composite indicates the intra-space between the LaV and F-BN sheets.

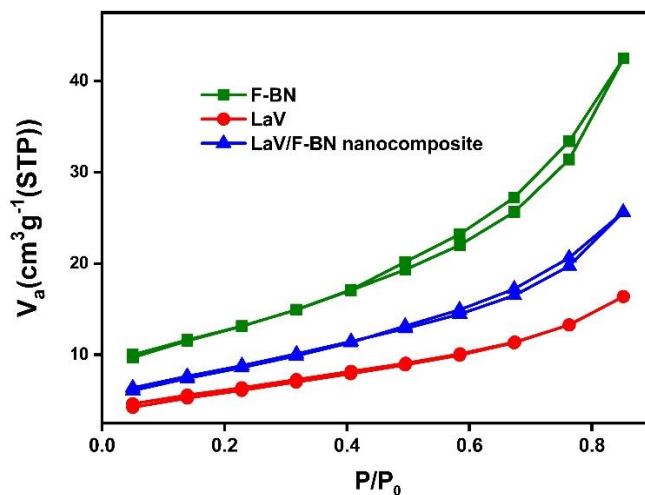


**Fig. S3** BET N<sub>2</sub> adsorption-desorption curves of LaV, F-BN and LaV/F-BN nanocomposite.

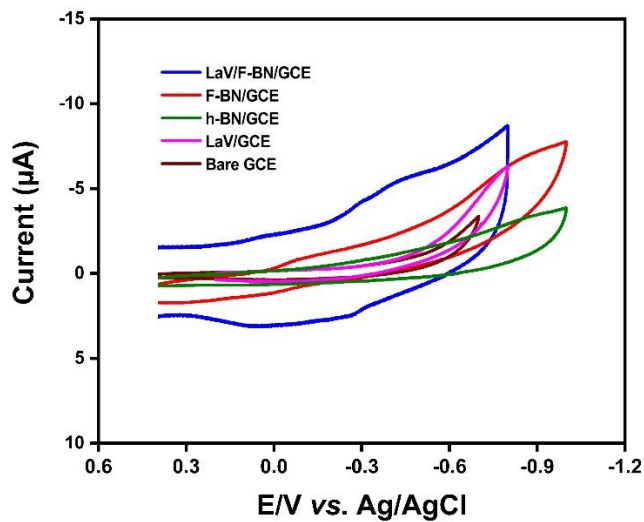


**Fig. S4** CV signals of bare and modified electrodes in the 0.05M PB (pH 7.0) without FZD.

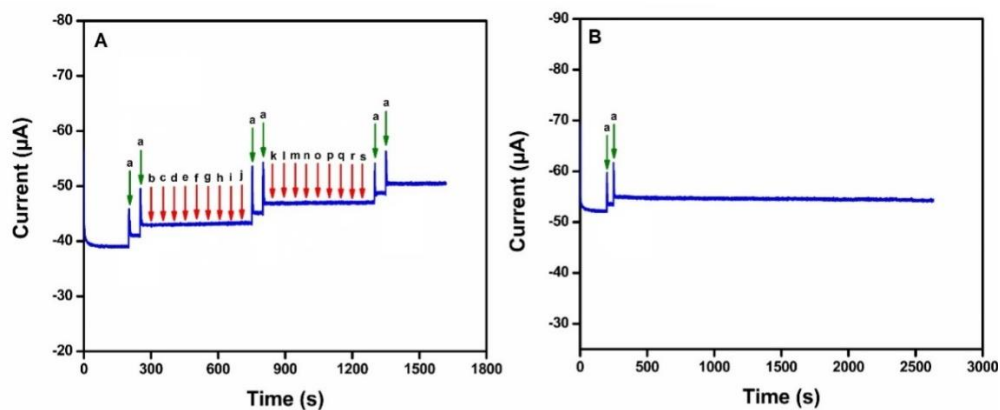


**Fig. S5** (A) Selectivity test of LaV/F-BN/RDGCE with the successive addition of 100  $\mu\text{M}$  FZD (a) and higher concentration of interfering species (b–s) in 0.05 M PB (pH 7.0). (B) The operational stability of the LaV/F-BN/RDGCE.

**Table S1** FZD detection in human blood serum and urine samples.

Samples	FZD Added	FZD Found	Recovery
	( $\mu\text{M}$ )	( $\mu\text{M}$ )	(%)
Human blood serum	–	–	–
	1.00	0.95	95.00
	2.00	1.97	98.50
	3.00	2.90	96.70
Human urine	–	–	–
	1.00	0.97	97.00
	2.00	1.95	97.50
	3.00	2.95	98.30